Organic & Biomolecular Chemistry

Accepted Manuscript

ROYAL SOCIETY OF CHEMISTRY

www.rsc.org/obc

Topochemical Polymerization of Unsymmetrical Aryldiacetylenes Supramolecule with Nitrophenyl Substituents Utilizing C–H···π Interactions

Shichao Wang[1], Yong Li[1], Hui Liu[1, 2], Jinpeng Li[1], Tiesheng Li[1 *], Yangjie Wu[1], Shuji Okada[3], and Hachiro Nakanishi[4]

[1]College of Chemistry and Molecular Engineering, The Key Lab of Advanced Information Materials of Zhengzhou, Zhengzhou University, Kexuedadao100, Zhengzhou 450052, P.R. China

[2]Department of Chemistry, Zhengzhou Normal University, Zhengzhou 450003, P.R. China

[3]Graduate School of Science and Engineering, Yamagata University 4-3-16 Jonan, Yonezawa 992-8510, Japan

[4]Institute of Multidisciplinary Research for Advanced Materials, Tohoku University 2-1-1 Katahira, Sendai 980-8577, Japan

Abstract

Diacetylenes are versatile building block in which many functional groups can be incorporated for the construction of new materials with desired properties. In this paper, 6-(*p* or *m*-nitrophenyl)-3, 5-heaxdiyne-1-ol (**4a**, **4b**) containing the nitrophenyl group (host) and 2-hydroxyethyl group (guest) in different terminals of diacetylenes were designed to establish an ordered supramolecular assembly that is commensurate with the strict requirement for topochemical polymerization of diacetylenes. Crystal film and bulk crystal of compound **4b** were obtained successfully by cast film and re-precipitation method. They both could photopolymerize to the corresponding regular poly(diacetylene) polymer, as evidenced by UV-vis, IR, FL spectra and Raman spectroscopy. Electrochemical properties and behaviors of **4a** and **4b** were also investigated, and it shows that the differences between para and meta position of mono-phenylacetylene substituent probably results from the topochemical polymerization. Thus, *m*-nitrophenylbutadiyne derivatives with sizeable C–H···π interactions seemed to be effective to form a polymerizable packing which is appropriate for the topochemical polymerization.

Keywords: diacetylene; self-assembly; supramolecule; topochemical polymerization

Introduction

Polydiacetylenes (PDAs) are unique conjugated polymers with a highly crystalline feature obtained by the solid-state topochemical polymerization of 1, 3-butadiynes[1] or diacetylene[2]. The moieties linking with diacetylene (DA) are versatile building block for the construction of molecular complexes, polymer composites and supramolecular structure[3,4], which is linear, rigid and conjugated to make it ideal for the placement of metal centers at precise distances from each other[5]. Similarly, diacetylenes have been used to connect various organic functionalities, including the linking of aromatic rings to extended conjugated structure or other structures[6,7], in which these conjugated structures have attracted much attention for applications[8-11]. The resulting polymers are highly conjugated, deeply colored and display important optical and non-linear optical properties and have potential applications as optical limiters and waveguides, and sensitivity to environmental changes that make them ideal candidates for the synthesis of chemical or biological sensors[12,13]. In addition to serving as a static scaffold, DAs could be useful for

engineering larger structures, such as oxidation resistance, temperature, mechanical properties and surface hardening of polymers upon incorporation[14,15].

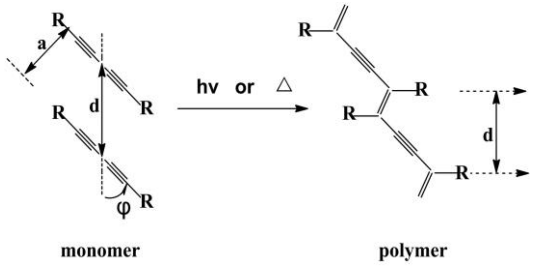

Scheme 1 The topochemical polymerization of DA. The values for 1, 4 addition polymerization are d ≈ 4.9 Å; φ ≈ 45°; a ≈ 3.5 Å

Despite these excellent properties, the design of DAs remains a challenge. In principle, this reaction is usually a photochemical process, though it also occurs thermally[16]. With only minimal packing rearrangements, DA monomers can be polymerized in the topochemical manner which the single crystals of the monomer can be transformed into polymer single crystals. The molecular alignment to satisfy topochemical polymerization is at least threefold (Scheme 1): first, the identity period d of the monomer is about 4.9 Å. Second, the distance a is at approximately 3.5 Å, which represents the van der Waals contact between adjacent molecules. Third, the inclination angle φ between the DA axe and translational vector is close to 45 °. The difficulty is that the vast majority of DA monomers do not crystallize in accordance with these structural parameters and undergo random 1,2- or 1,4-polymerization, which resulted in unknown disordered polymer material. Empirically, the appearance of an intense blue color that corresponds to a maximum absorption wavelength of 640nm generally mean that the packing parameters of the monomer crystal meet geometrical criteria as shown in scheme 1[17]. Interestingly, responding to environmental stimulations, a phase transition (blue-to-red) of PDAs occurs.

If a given DA does not crystallize properly, we can adopt other ways to change the crystal structure, such as Langmuir-Blodgett technology[18-20], copolymer[21] and pressure-catalyzed polymerization[22]. Through these approaches mentioned above, the DAs might have a structure which matches the requirement for regular polymerization, but all of these operations are complexes. The traditional way is the directly design of the monomer structure through amide groups[23], fluorine containing phenyl groups[24], perfluorophenyl-phenyl groups[25] and so on. Especially, C–H···π and π···π interactions as a wide array of supramolecular phenomena in biology and chemistry can also be used for the structure design. In addition to this, aryl-substituted PDAs have been of considerable interest[26, 27], because they offer a way to extend the conjugation of the polymer onto the side chains and, consequently, enhancing the photoelectric properties of such architectures. In this connection, several monophenylbutadiyne derivatives with simpler structures were investigated[28]. However, no topochemical polymerization was confirmed.

This solution is simple to implement, but it is hardly predictable. First, various intramolecular forces must be considered. Second, the difficulties in topochemical polymerization of aryldiacetylenes are attributed to the rigidity of aromatic pedant groups because of movement of the rigid ring which may just be too disruptive for the crystal lattice to remain intact which was proved by both Lando's and Nakanishi's results[29]. Lauher proposed that perhaps an unsymmetrical aryldiacetylene could provide an alternate route to the preparation of PDA single crystals[30]. The remaining required design element is an appropriate set of matched substituents that will assure a strong intermolecular interaction between adjacent molecules. In order to establish a crystalline lattice commensurate with the repeat distance of the desired polymer, our effort is made to develop rational and simple design for the preparation of DAs, in which mono-aryl containing electro-withdrawing group (host) and 2-hydroxyethyl group (guest) in different terminals of DAs, with which these molecules are expected to be gotten in predictable structures based upon self-assembly via hydrogen bonds[31] and aromatic ring stacking[25].

In this paper, designed 6-(*p* or *m*-nitrophenyl)-3,5-heaxdiyne-1-ol(**4a**,**4b**) compounds were synthesized and characterized with ^{1}H NMR, ^{13}C NMR, IR, and GC/MS spectra. Solid-state polymerization properties of compound **4a** and **4b** were also systematic investigated by deep UV irradiation and annealing. Cast film and re-precipitation method were applied to align crystal structure appropriately for the topochemical polymerization. Crystal film and bulk crystal of compound **4b** were obtained successfully and photopolymerized to the corresponding regular PDA polymer, as evidenced by UV-vis, IR, FL spectra and Raman spectroscopy, as well as single-crystal structure analysis. Obviously, once our strategy is proved to be successful in preparing aryl-substituted PDAs, nitrophenylbutadiyne derivatives seem to be effective to form a polymerizable packing which is appropriate for a topochemical polymerization and other more complex nitrophenyl-substituted PDAs will be tested.

Experimental

Synthesis of diacetylene derivatives 4a and 4b

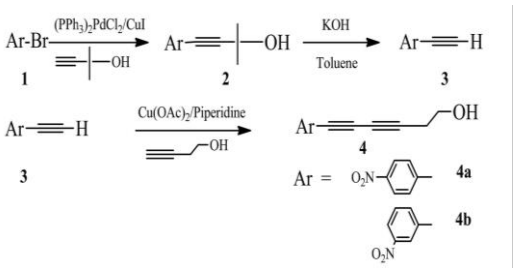

Scheme 2 Synthetic procedure of **4a** and **4b**.

6-(*p* or *m*-nitrophenyl)-3, 5-heaxdiyne-1-ol (**4a**, **4b**) were synthesized according to the route as shown in Scheme 2. Preparation of **2**, **3** has been reported previously[32]. **4a** and **4b** that were not reported before were obtained by the asymmetric coupling reaction of **3** with 3-butyn-1-ol, using $Cu(OAc)_2$ as a catalyst.

In a 50 mL three-neck round-bottom flask fitted with O_2 inlet and outlet, 0.147g of 3-nitrophenyl acetylene (1mmol) in 20mL of dichloromethane was added. Piperidine (0.3mL, 3mmol) were added, followed by 0.018g $Cu(OAc)_2$ (0.1mmol) to it under ice. The reaction solution was stirred throughout at room temperature and was monitored by TLC. The reaction was found to be complete after 8h. The solution were abstracted with dichloromethane followed by wishing with NH_4Cl and water, The compound was passed through a silica gel column using petroleum ester/ethyl acetate (2:1) as eluent and **4a** and **4b** were obtained.

4a: Yellowish solid, yield: 65%, Mp: 120-122 ℃, IR (KBr pellet, cm^{-1}): 3262, 3103, 2929, 2236, 1922, 1592, 1515, 1343, 1048, 852; ^{1}H NMR (400MHz, $CDCl_3$): δ 8.17-8.19 (d, J=8.8Hz, 2H, -C_6H_4), 7.59-7.62 (d, J=8.8Hz, 2H, -C_6H4), 3.81-3.84(t, J=6.4Hz, 2H, -CH_2-OH), 2.66-2.69(t, J=6.0Hz, 2H, ≡C-CH_2-), 1.872(s, 1H, -OH); ^{13}C NMR(100 MHz, $CDCl_3$): δ 147, 133, 128, 123, 84, 79, 73, 66, 60, 24; MS: 214 $[M-1]^+$

4b: Yellowish solid, yield:63%, Mp: 70-72 ℃, IR (KBr pellet, cm^{-1}): 2958, 2925, 2855, 2236, 1733, 1635, 1531, 1458, 1351, 1261, 1089, 1042, 863, 801, 735; ^{1}H NMR (400MHz, $CDCl_3$): δ 8.30-8.31(t, J= 2.0Hz, 1H, -C_6H_4), 8.17-8.20(m, 1H, -C_6H_4), 7.74-7.77(m, 1H, -C_6H_4), 7.48-7.52(t, J=8.0Hz, 1H, -C_6H_4), 3.81-3.84(t, J=6.4Hz, 2H, -CH_2-OH), 2.65-2.68(t, J=6.0Hz, 2H, ≡C-CH_2), 1.861(s, 1H, -OH); ^{13}C NMR(100 MHz, $CDCl_3$): δ 148, 138, 129, 127, 124, 82, 72, 66, 60, 23; MS: 214$[M-1]^+$

Preparation of cast film and crystal prepared by re-precipitation

Cast film and crystal prepared were depicted in Scheme 3.

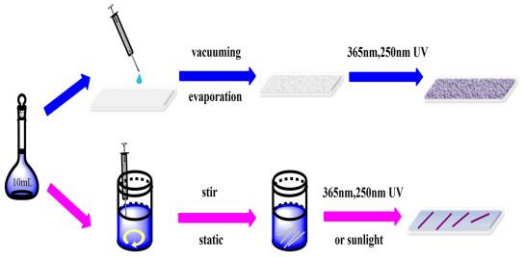

Scheme 3 Schematic route for preparation of **4a** or **4b** cast film (up) and crystals via re-precipitation (low).

4a or **4b** monomer was added to a flask containing chloroform. The solution was stirred for 20 min and then the resulting solution was filtered through a 0.2μm Teflon filter and was casted onto quartz slides. Cast films were dried for 16 h in a vacuum at room temperature.

10 mg/mL **4a** or **4b** acetone solution (1 mL) was injected into vigorously stirred super pure water (3mL) at ambient temperature to give crystal dispersion. The dispersion solution was put in static for some time. Only **4b** crystals were collected with size ranging from 1cm to well over 3cm and width from 100 to 200μm[33].

Results and discussion

In the synthesis process of compound **4b**, an unexpected purple solid insoluble in common laboratory solvents appeared in **4b** solution after chromatographic purification. However, monomer **4a** and **4b** were obtained as yellow solid after vacuum and turned to a large number of deep yellow soluble oligomers (**poly-4a**, **poly-4b**) upon UV irradiation. Polymer molecular weight was obtained by gel permeation chromatography analysis (Table S1). A large polymerization degree about 70 was found in **poly-4b**, which meant polymer materials with disordered extended π-conjugation system were obtained. Similarly, the high concentration liquid film without vacuum process was attempted to undergo UV irradiation, a yellow liquid oligomers appeared. However, their structures are not regular PDAs, as evidenced by the absence of new UV-vis absorption in visible region (Figure S1, S2).

Therefore, cast film and re-precipitation method were applied to align crystal structure appropriately for the topochemical polymerization. Crystal film and bulk crystal of compound **4b** were obtained successfully and polymerized to the corresponding regular PDA polymer. Color changes of **4b** cast film and crystals prepared by re-precipitation were presented in Figure 1. In the case of **4b** cast film, it is well-known that the molecular packing in thin films can significantly differ from the bulk crystal structures[34]. It is worth mentioning that the casting solution must be freshly prepared, and the vacuum process was necessary for the formation of crystal film.

We found it more difficult to form large crystals of **4b**. Nevertheless, colorless long needle-shaped crystals formed by re-precipitation with slow vaporation/crystallization over several days and became red during UV irradiation at 365nm as shown in Figure 1c, 1d.

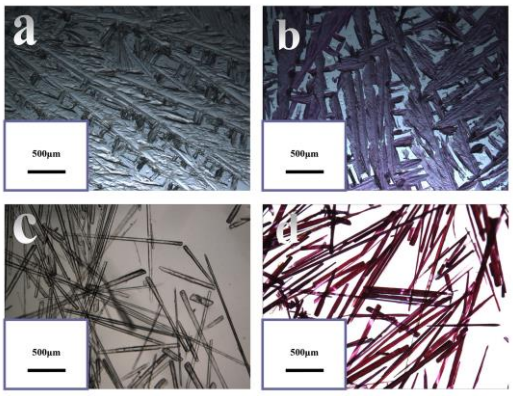

Fig. 1 Optical micrograph of **4b** cast film (a, b) and **4b** crystal prepared by re-precipitation (c, d) before and after deep UV irradiation at 250nm or 365nm UV light for 15min.

It is important that how about the yield of polymer obtained by re-precipitation method. Therefore, UV irradiation of the crystals **4b** led to the conversion into a red insoluble material. However, UV light could not penetrate through the crystals due to polymers produced on their surfaces. The pure polymer **4b** was obtained as fiber like about 12.2% yield after Soxhlet extraction of residual monomer with dichloromethane (DCM) after deep UV irradiation for 1.5h. The optical micrograph and scanning electron microscope (SEM) image of polymer were shown in Figure 2.

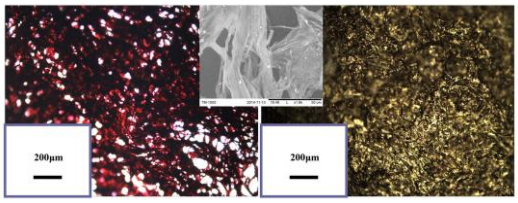

Fig. 2 Optical micrograph (transmission (left) and reflection (right)) of polymer after Soxhlet extraction. The inset shows SEM image.

Crystal Structure of 4b

Several attempts were made to obtain **4a** single crystals, but these efforts were unsuccessful. Eventually, an X-ray diffraction analysis (XRD) of **4a** solid was undertaken. A detailed description was provided in the XRD section. However, **4b** single crystals were very simple to obtain. When pure **4b** is recrystallized from an acetone/water, crystals formed that showed an unexpected appearance in blue color.

A well-formed crystal was selected, and a structure determination revealed that the molecule had crystallized as a triclinic with alignment of the diacetylene functionalities in a bit reasonable agreement with the requirements for a topochemical polymerization.

The crystal structure of **4b** monomers was investigated on the basis of the results of the X-ray single-crystal structure analysis (Figure S3). Single crystal X-ray diffraction reveals that **4b** monomers crystallizes in the triclinic space group P-1 and exhibits an alignment of the DA functionalities. As shown in Figure 3a, the carbon-carbon distance for 1, 4-propagation during polymerization is 3.65Å [35]. It should be pointed out that there are aromatic ring systems and heteroatoms in **4b** which may form various hydrogen bonds stacking interactions. Analysis of the crystal packing of **4b** revealed that an infinite 2-D supramolecular network was formed by two intermolecular hydrogen bonds interactions (Figure 3b). One is the O–H···O hydrogen bonds interactions. The O···O distances are 2.980Å, the bond angles around O–H···O are 167°. The other is the C–H···O hydrogen bonds, which play important roles in biological carbohydrate-protein recognition systems[36-38]. The H···O distances of hydrogen bonds are 2.362Å (bond angles around C–H···O are 162.95°) between the activated C-H groups of benzene rings and the hydroxy O-atoms, which are shorter than the approximate distance (d, 2.49-2.74Å) of the H···O reported by Desiraju et al.[39, 40]. These 2-D layers are further connected to 3-D supramolecular network (Figure 3d) by the edge-to-face C–H···π interactions (distance 3.365Å, dihedral angel 91.3°, H/π-plane separation: 3.323Å) between adjacent phen ring of **4b** which leaded to a layered stacking along the a-axis of the crystal (Figure 3c)[41,42]. These foregoing facts specified that the weak interactions are very important in **4b**, where they contributed significantly to molecular self-assembly processes.

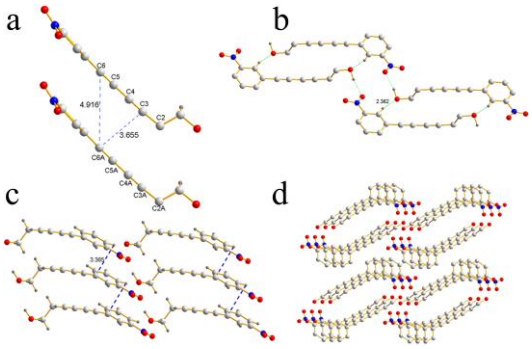

Fig. 3 (a) Stacking diagram of **4b** drawn at 20% probability. (b) Two-dimensional layered supramolecular network of **4b**. The dashed lines represent hydrogen bonds interactions. (c) The edge-to-face C–H···π interactions along the a-axis. (d) Stacking diagram of **4b**. Part hydrogen atoms are omitted for clarity.

Data of the molecule crystal revealed that it was in a bit reasonable agreement with the requirements for a topochemical polymerization and slow formation of an amount of insoluble material was observed.

Solid-state Polymerization of 4b cast film and bulk crystal

The photopolymerization of the DA monomers was carried out in the solid state under UV irradiation at 250nm or 365nm. The process of photopolymerization was confirmed by a color change in the appearance of the crystal, in which the color of PDAs is due to a π-π* transition of the linear-conjugated polymer backbone. Unpolymerized DAs do not exhibit absorption in the visible region, but upon polymerization a blue color appears from two absorption band with maximum around 590nm and 540nm shown in Figure 4. In the case of irradiation at 365nm, the absorption had developed an intense absorption band with a maximum at about 590nm (Figure 4). The relatively sharp absorption band at 590nm can be attributed to a band of a "purple form", intermediate in order between the blue phase and the red phase[43]. The position and width of the second, broader band at about 540nm is likely that this should be assigned to PDA groups in a less ordered environment, in a so-called "red phase"[44]. In order to investigate the irradiation dependence of the absorption spectra, **4b** cast film irradiated at 365nm was carried out for different time, and then the UV-vis absorption spectra were recorded at ambient without

the separation of the resulting polymer and the remaining monomer as shown in Figure S4, in which the absorbance of typical peaks of conjugated backbone increased with increasing irradiation time and became broader with new shoulder peak at about 650nm. It is indicating that regular 1, 4-addition occurred[45].

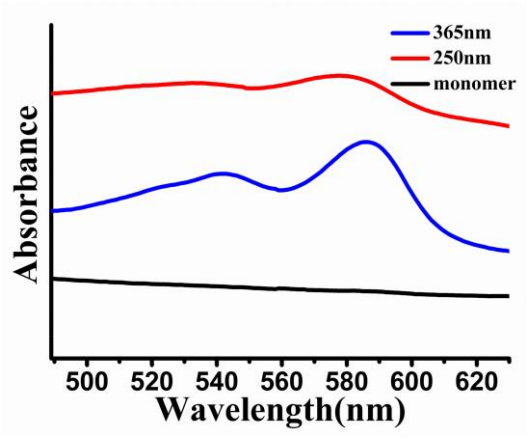

Fig. 4 UV-vis spectrum of cast film on quartz before (black) and after (red, blue) irradiation at 250nm and 365nm for 10min, respectively.

This also can be confirmed by FL spectra. Fluorescence spectra of **4b** solution, cast film and cast film irradiated by deep UV light were also investigated. In the case of **4b** solution, the fluorescence emission spectra at λ_{exc}=380nm as shown in Figure S5(d), in which the emission band was at about 440nm. There is inconspicuous emission peak at λ_{exc}=250nm as shown in Figure S5(e). However, stronger emission peak of **4b** cast film irradiated by deep UV light at 400 nm and 580nm at λ_{exc} = 250nm could be observed in Figure S5(f). After UV irradiation for a long time, the fluorescence disappeared. Nevertheless, the bulk crystals obtained by re-precipitation method had no fluorescence throughout UV irradiation process, which may result from the fluorescence quenching effect of nitrobenzene group. It is well known that PDAs have different fluorogenic properties between a red fluorescent state and a blue non-emissive state[46]. It might seem that different preparation methods led to different polymer forms. The difference of compound structure may have an effect on fluorescence properties. Thus, unlike most PDAs that exhibit thermochromism properties, the achievement of a controlled transformation between red and blue state is worth investigating as future works.

To confirm the formation of PDAs on the quartz substrate, we used Raman spectrum to probe the changes before and after UV irradiation. As shown in Figure 5a, the acetylene stretching band appeared at 2239cm^{-1}. After UV irradiation of **4b** cast film, two new peaks at 1458cm^{-1} and 2089cm^{-1} at a much greater intensity assigned to the typical conjugated alkyne−alkene structures of PDA (Figure 5b)[47]. The result evidenced that **4b** cast film transformed to PDAs by UV irradiation.

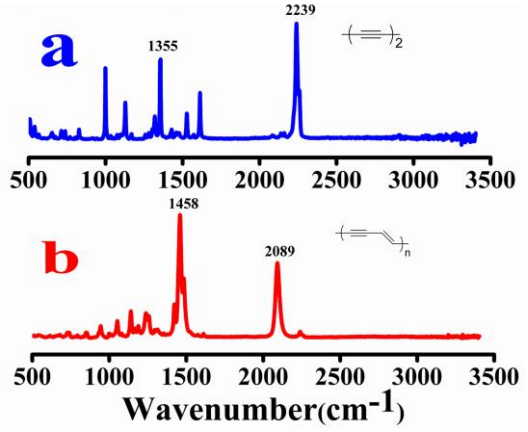

Fig. 5 Raman spectra of cast film on quartz before (a) and after (b) irradiation at 365nm for 100min.

There are little changes in 2212cm^{-1}, 2217cm^{-1} corresponding to stretching vibration of acetylene and double bond when irradiated by 250nm in its IR spectra of **4b** cast film on CaF_2 substrate (Figure S6b). The bands at 1353cm^{-1} of the symmetric -NO_2 stretching became weak and extended to the long wavelength region, in which it proved that polymerization took placed with extension of π-conjugation, leading to the change of nitro group (Figure S6c). It can be plausibly explained that the orientation of molecular in crystal changed by polymerization procession which resulting in the orientation of nitro-group.

Those results which are consistent with structure analysis of **4b** single crystal showed that a prerequisite of the regular polymerization is highly ordered packing of monomers. That is to say that the polymerization successfully proceeds because the

monomer spacing, imposed by the hydrogen bond forces between the hydroxyl with nitro groups in different molecules, which made molecular close enough to the spacing required for the DA backbone to form PDA.

Heat experimental

Heating the same fresh single crystal to a temperature of 60℃ by a slow annealing treatment without light for 1h gave no polymer. However, when crystals were kept under ambient light at room temperature, appropriately aligned monomer crystals will polymerize spontaneously. As the heating temperature is increased until at 70℃ under the light, the crystal began to melt and expanded, but the polymerized part is still maintaining the same shape like crystal as shown in Figure S7.

Water contact angle analysis

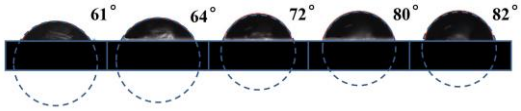

Fig. 6 Static water contact angle of **4b** cast film irradiated at different time. (a), 0min;(b), 10min;(c), 20min;(d), 30min;(e), 45min.

A CAMERAY digital color CCD camera was used for the measurement of the contact angle of water droplets on the surface of **4b** cast film irradiated by UV light. A small droplet was placed on the surface of substrate and vibrated gently to overcome any contact line pinning effects. Then it gave a uniform contact angle at all points along the three phase contact line. Water droplets deposited on solid surfaces were shown in photo images (Figure 6). The contact angle was as low as 5° for the hydrophilic glass substrate by hydrophilicity treated, which showed that the glass substrate had good hydrophilic activity. On the case of cast film of **4b**, the contact angle increased from 61° to 82° (Figure 6 a-e), indicating that the surface configuration had a significant change due to the photopolymerization of **4b,** which is consistent with the results of SEM (Figure S8). As shown in Figure S8, the surface of **4b** cast film became rough after UV irradiation for 20 minutes.

XRD analysis

X-ray diffraction (XRD) patterns of compound **4a**, **4b** were measured to study the packing configuration and the distances within the supramolecular structure and compare different solidified forms. Samples were obtained through usual solidified form (**4a-u**, **4b-u**), cast film (**4b-c**) and re-precipitation (**4b-r**) (Figure 7).

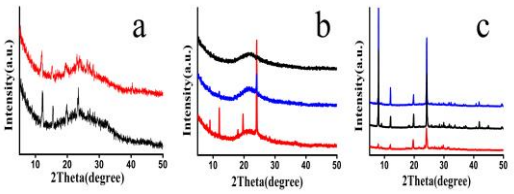

Fig. 7 X-ray diffraction patterns of a) **4a** obtained through usual solidified form. The black and red lines are for **4a-u** before and after UV irradiated at 250nm, respectively. b) **4b** cast film. The red, blue, and black lines are for **4b-c**, **4b-c** after UV irradiation and **4b-c** after washed by acetone, respectively. c) **4b** bulk crystal prepared by re-precipitation. The black and blue lines are for **4b-r** prepared by re-precipitation before and after irradiated at 250nm, respectively. The red line in (c) is for **4b-u**.

The crystallinity of **4a** obtained through usual solidified form was low while **4b** obtained by same way showed several sharp peaks, which also confirmed that **4b** had more regular intermolecular interactions(Figure 7a, 7c). The insufficient crystallinity of **4a** (Figure 7a) may cause irregular alignment of the butadiyne group resulting in a low polymerization degree (Table S1), which may be associated with its weak C–H···π interactions. As shown in Figure 6b, although **4b** cast film were confirmed to be amorphous by the broad diffraction peaks at 2θ=22°, several peaks implied partial regular structures[28]. After UV irradiation and washed by acetone, the crystallinity of **4b** cast film was almost lost and completely amorphous, respectively. Similar sharp peaks at 2θ=24° (3.67Å) attributed to the π–π distance between the molecules have been observed in different solidified forms (Figure 7b, 7c)[48]. Distinctively, **4b** bulk crystal prepared by re-precipitation showed a particularly sharp and intense peak at 2θ=8° (11.05Å), which is very close to a lattice constant c (11.29Å) of **4b** single crystal. The similar peak before and after UV irradiation also

revealed that the bulk crystals have not undergone a phase change to a new form (Figure 7c).

Electrochemical analysis

Analysis by UV-vis spectra and Raman spectroscopy has been able to reveal the topochemical polymerization of compound **4b**. The introduction of the redox-active nitrobenzene groups further allows us to perform a cyclic voltammetry (CV) study to provide more detailed insight into the relationship between regular topochemical polymerization and irregular polymerization. The 80wt% prepared samples were mixed with 15wt% acetylene black and 5wt% polytetrafluoroethylene (PTFE) in aqueous solution to form slurry and then cast onto nickel foams followed by drying at 30℃ for about 12h[49][50]. After compressed, nickel foams containing samples were used as working electrode.

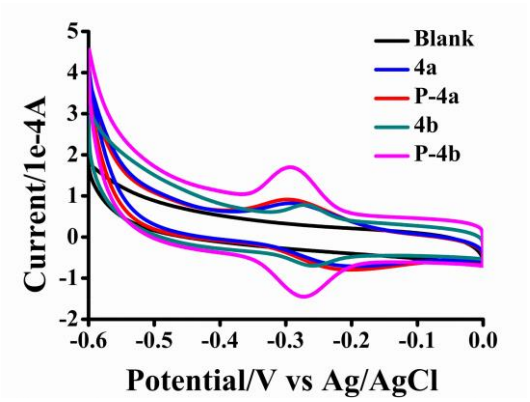

Fig. 8 Cyclic voltammograms of nickel foams(Blank), **4a** powders before(**4a**) and after(**P-4a**) UV irradiation, and **4b** crystal before(**4b**) and after(**p-4b**) UV irradiation in aqueous solution with 0.2 M KCl. Initial and final potentials, 0V; reversal potential, -0.6V; scan rate, 50 mV s^{-1}.

As shown in Figure 8, the initial scan in the CV from 0 to -0.6V show the only one well-defined and stable redox waves, which correspond to the reduction of the nitrobenzene group and the reoxidation of the nitrobenzene radical anion[51]. The CV curves of **4a** powders before and after UV irradiation (**4a** and **P-4a**) only showed a negligible change. However, The peak current and peak potential of **4b** crystal before and after UV irradiation (**4b** and **P-4b**) showed the dramatical change, which may be associated with the changes of electroactivity and crystal structure.

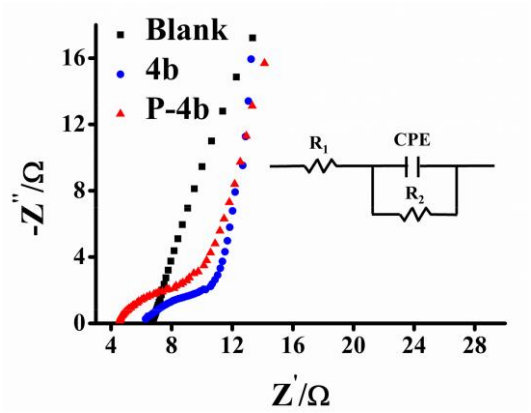

Fig. 9 Nyquist plots of nickel foams (Blank), **4b** crystal before (**4b**) and after (**p-4b**) UV irradiation. The inset is the equivalent circuit model. R_1 and R_2 are system resistances and charge-transfer resistances, respectively. CPE is the constant phase element.

To gain insight into the prominent change of electrochemical behavior of **4b** observed from CV, ac impedance measurements were performed. As shown in Figure 9, a frequency range of 0.1-10^5Hz with signal amplitude of 20mV was employed and nyquist spectra showed a semicircle in the high-frequency range and a straight ascending line in the low-frequency range. The equivalent circuit model of the studied system is also shown in Figure 9 according to the works of others[52][53]. R_1 corresponds to the resistance of the surface coating formed on the nickel foams and R_2 represents the ability to impede ion transport at the electrode/electrolyte interface[54]. It can be seen that **P-4b** exhibits a smaller R_1 (4.245Ω) and R_2 (9.654Ω) than **4b** (5.953Ω, 10.62Ω), which may be caused by the extended conjugation after polymerization (Table S2). Topochemical polymerization process significantly influences the electrochemical behavior, which is different from irregular polymerization based on our results of electrochemistry analysis.

Conclusions

6-(*p* or *m*-nitrophenyl)-3, 5-heaxdiyne-1-ol (**4a**, **4b**) were designed and characterized with ^{1}H NMR, ^{13}C NMR, IR, and GC/MS spectra. The mono-aryl containing electro-withdrawing group (host) and 2-hydroxyethyl group (guest) on different terminals of compound **4a**, **4b** made them easy to self-assembly to form crystals by numerous O–H···O and C–H···π

interactions, while the obtained poly(diacetylene)s with aromatic rings as a host group directly bound to the alternating ene–yne main chain gave an extension of the π-conjugation system. Solid-state polymerization properties of compound **4a** and **4b** were also systematic investigated by deep UV irradiation and annealing, in which only compound **4b** showed that it could polymerize to give a blue-colored polymers insoluble in common laboratory solvents. Cast film and re-precipitation methods were applied to align crystal structure appropriately for the topochemical polymerization. Crystal film and bulk crystal of compound **4b** were obtained successfully. They both could photopolymerize to the corresponding regular poly(diacetylene) polymer, as evidenced by UV-vis, IR, FL spectra and Raman spectroscopy, as well as single-crystal structure analysis of **4b** single crystals in which a crystalline lattice nearly commensurate with the repeat distance of the desired structure for regular polymerization. Electrochemical properties and behaviors of **4a** and **4b** were also investigated, and it shows that the differences between para and meta position of mono-phenylacetylene substituent probably results from the topochemical polymerization. Thus, m-nitrophenylbutadiyne derivatives with sizeable C–H···π interactions seemed to be effective to form a polymerizable packing which is appropriate for the topochemical polymerization.

Acknowledgements

This work was partially supported by the Fund of Nature Science of Henan Provence (112102210215), Prof. Zhi Ma for Raman spectra and Lu Zhu for XRD analysis.

Notes and references

1 Wegner, G.; A. Naturforsch. *Teil B* 1969, **24**, 824–832.

2 Bloor D, Chance R. R. NATO ASI Series, Series E, Applied Science, 102; Martinus Nijhoff: Dordrecht, The Netherlands, 1985.

3 Isabelle Levesque; Simon Rondeau-Gagné; Jules Roméo Néabo and Jean-François Morin. *Org. Biomol. Chem.* 2014, 12, 9236–9242.

4 Jianzhao Liu; Jacky W. Y. Lam; Ben Zhong Tang. *Chem. Rev.* 2009, **109**, 5799–5867.

5 Li Liu; Zuxing Chen; Shizhong Liu. *Acta Chim Sinica.* 2006, **64(9)**, 884-888.

6 Te-Jung Hsu; Frank W. Fowler; Joseph W. Lauher. *J. Am. Chem. Soc.* 2012, **134(1)**, 142–145.

7 Kenneth W. Muir; David G. Morris; Karl S.Ryder; Shirley Walkera. *CrystEngComm* 2004, **6(48)**, 280–283.

8 Tiesheng Li; Okada S; Nakanishi H. *Polymer Bulletin* 2003, **51**, 1003-1010.

9 Kenichi Morigaki; Holger Schönherr; Takashi Okazaki. *Langmuir* 2007, **23(24)**, 12254–12260.

10 Hye Jin Park; Jong-Man Kim. *Appl. Mater. Interfaces* 2013, **5 (17)**, 8805–8812.

11 Toru Odani; Shuji Okada; Chizuko Kabuto, et al. *Crystal Growth & Design* 2009, **9(8)**, 3481-3487.

12 L. Bredas; C. Adant, P. Tackx; A. Persoons. *Chem. Rev.* 1994, **94**, 243-278.

13 Masaki Murata; Takeo Hoshi; Isao Matsuoka; Takuya Nankawa;, Masato Kurihara; Hiroshi Nishihara. *Journal of Inorganic and Organometallic Polymers* 2000, **10(4)**, 209-219.

14 Yang Song; Liana M. Klivansky, et al. *Langmuir* 2011, **27**, 14581–14588.

15 Sumrit Wacharasindhu; Suriyakamon Montha; Jasuma Boonyiseng, et al. *Macromolecules* 2010, **43**, 716–724.

16 H. M. Barentsen; M. van Dijk; H. Zuilhof; E. J. R. Sudholter. *Macromolecules* 2000, **33**, 744-766.

17 R. H. Baughman; K. C. Yee. J. *Polygr. Sci. Macromol.* Rev. 1978, **13**, 219-239.

18 Ling Zhong; Xuefeng Zhu; Pengfei Duan, et al. *J. Phys. Chem. B* 2010, **114**, 8871–8878.

19 Xiaoping Nie; Guijun Wang. *J. Org. Chem.* 2006, **71**, 4734-4741.

20 Anu Puri; Hyunbum Jang; Amichai Yavlovich, et al. *Langmuir* 2011, **27**, 15120–15128.

21 Rui Xu; Volker Gramlich; Holger Frauenrath. *J. Am. Chem. Soc.* 2006, **128 (16)**, 5541–5547.

22 Tanaka, Y.; Iijima, S. I.; Shimizu, T.; Fujikawa, H.; Matsuda, H.; Nakanishi, H.; Kato, M.; Kato, S. I.. *J. Polym. Sci. Part C: Polym. Lett.* 1986, **24**, 177-184.

23 Jong Man Kim; Ji-Seok Lee; Hyun Choi; Daewon Sohn; Dong June Ahn. *Macromolecules* 2005, **38**, 9366-9376.

24 Shuji Okada; Minoru Ohsugi; Atsushi Masaki ; Hiro Matsuda; Shigeru Takaragi; Hachiro Nakanishi. *Mof. Cryst. Liq. Cryst.* 1990, **183**, 81-90.

25 Rui Xu; W. Bernd Schweizer; Holger Frauenrath. *J. Am. Chem. Soc.* 2008, **130**, 11437–11445.

26 Sarkar, A.; Okada, S.; Matsuzawa, H.; Matsuda, H.; Nakanishi, H. *J. Mater. Chem.* 2000, **10**, 819–828.

27 Hui Liu; Huanhuan Li; Tiesheng Li; Yong Li; Yangjie Wu; Shuji Okada; Hachiro Nakanishi. *Journal of Organometallic Chemistry* 2014, **767**, 144–149.

28 Jun-ichi Watanabe; Harumi Yokoyama; Shuji Okada; Shigeru Takaragi; Hiro Matsuda; Hachiro Nakanishi. *Mol. Cryst. Liq. Cryst.* 2009, **505**, 203-209.

29 Matsuda, H.; Nakanishi, H.; Hosomi, T.; Kato, M. *Macromolecules* 1988, **21**, 1238–1240.

30 Zhong Li; Frank W. Fowler; Joseph W. Lauher. *J. Am. Chem. Soc.* 2009, **131**, 634–643.

31 Yuh-Loo Cbang; Mary-Ann West; Frank W. Fowler; Joseph W. Lauher. *J. Am. Chem. Soc.* 1993, **115**, 5991-6000.

32 Sarkar A.; Okada S.; Komatsu K.; Nakanishi H.; Matsuda H. *Macromolecules*, 1998, **31**, 5624-5630.

33 Tiesheng Li; Shuji Okada; Hirohito Umezawa; Hitoshi Kasai; Hachiro Nakanishi; Satya S. Talwar; Tatsumi Kimura; Hiro Matsuda. *Polymer Bulletin* 2006, **57**, 737–746.

34 Lei Zhang; Nicholas S. Colella; Feng Liu; Stephan Trahan; Jayanta K. Baral; H. Henning Winter; Stefan C. B. Mannsfeld; Alejandro L. Briseno. *J. Am. Chem. Soc.* 2013, **135**, 844−854.

35 Akikazu Matsumoto. *Top Curr Chem*. 2005, **254**, 263–305.

36 P. W. Baures; A. Wiznycia; A. M. Beatty. *Bioorganic & Medicinal Chemistry* 2000, **8**, 1599-1605.

37 Yael Mandel-Gutfreund; Hanah Margalit; Robert L. Jernigan; Victor B. Zhurkin. *J. Mol. Biol.* 1998, **277**, 1129-1140.

38 Sudha Anand; Anand Anbarasu; Rao Sethumadhavan. *Appl. Biochem. Biotechnol* 2009, **159**, 343–354.

39 Desiraju, G. R.; Steiner, T. Oxford University Press: Oxford 1999.

40 Ram Thaimattam; Feng Xue; Jagarlapudi A. R. P. Sarma; Thomas C. W. Mak; Gautam R. Desiraju. *J. Am. Chem. Soc.* 2001, **123**, 4432-4445.

41 Jinpeng Li; Huan Sun; Qinqin Yuan; Xiaoli Gao; Shaomin Wang; Yanyan Zhu; Lu Liu; Songhe Zhang; Yanan Zhang; Yuexin Guo; Baoxian Ye; Yaru Liu; Hongwei Hou; Yaoting Fan; Junbiao Chang. *Journal of Coordination Chemistry* 2013, **66(10)**, 1686-1699.

42 Jinpeng Li; Xiaofang Li; Huijuan Lü; Yanyan Zhu; Huan Sun; Yuexin Guo; Zhifang Yue; Jin'an Zhao; Mingsheng Tang; Hongwei Hou; Yaoting Fan; Junbiao Chang. *Inorganica Chimica Acta* 2012, **384**, 163–169.

43 Okada, S.; Peng, S.; Spevak, W.; Charych, D. *Acc. Chem. Res.* 1998, **31**, 229–239.

44 Carpick, R. W.; Sasaki, D. Y.; Marcus, M. S.; Eriksson, M. A.; Burns, A. R. *J. Phys.: Condens. Matter* 2004, **16**, R679-697.

45 Keisuke Kuriyama; Hirotsugu Kikuchi; and Tisato Kajiyama. *Langmuir* 1996, **12**, 6468-6472.

46 Dong June Ahn, Jong Man Kim. *Acc. Chem. Res.* 2008, **41**, 805-816.

47 Xu, Y. W.; Smith, M. D.; Geer, M. F.; Pellechia, P. J.; Brown, J.C.; Wibowo, A. C.; Shimizu, L. S. *J. Am. Chem. Soc.* 2010, **132**, 5334-5335.

48 Jules Roméo Néabo; Simon Rondeau-Gagné; Cécile Vigier-Carrière; Jean-François Morin. *Langmuir* 2013, **29**, 3446-3452.

49 Xiaobo Wang, Yong Yan, Bo Hao, and Ge Chen. *Appl. Mater. Interfaces* 2013, **5**, 3631-3637.

50 Youqi Zhu, Huizi Guo, Huazhang Zhai, and Chuanbao Cao. *Appl. Mater. Interfaces* 2015, **7**, 2745-2753.

51 Mie Lillethorup, Kyoko Shimizu, Nicolas Plumeré, Steen U. Pedersen, and Kim Daasbjerg. *Macromolecules* 2014, **47**, 5081-5088.

52 Shubin Yang, Xinliang Feng, and Klaus Müllen. *Adv. Mater.* 2011, **23**, 3575-3579.

53 Yuezeng Su, Shuang Li, DongqingWu, Fan Zhang, Haiwei Liang, Pengfei Gao, Chong Cheng, and Xinliang Feng. *Acs Nano* 2012, **6(9)**, 8349-8356.

54 Yuzhen Han, Pengfei Qi, Xiao Feng, Siwu Li, Xiaotao Fu, Haiwei Li, Yifa Chen, Junwen Zhou, Xingguo Li, and Bo Wang. *Appl. Mater. Interfaces* 2015, **7**, 2178-2182.

Table of contents entry

Synthesis and solid-state polymerization of unsymmetrical aryldiacetylenes supramolecule with nitrophenyl substituents